



23rd International Conference on Material Forming (ESAFORM 2020)

A Study on Microstructural Evolution in Cold Rotary Forged Nickel-Superalloys: C263 and Inconel 718

Paranjayee Mandal^{a,*}, Himanshu Lalvani^a, Kyle Watt^a, Alastair Conway^a, Martin Tuffs^b

^aAdvanced Forming Research Centre, University of Strathclyde, Glasgow, 85 Inchinnan Drive, PA4 9LJ, UK

^bRolls-Royce, Derby, DE24 8BJ, UK

* Corresponding author. Tel.: +44-0141-534-5616. E-mail address: paranjayee.mandal@strath.ac.uk

Abstract

C263 and Inconel 718 are precipitation hardenable nickel-superalloys widely used in different sections of a gas turbine engine dependent on their strength and temperature capability. Cold rotary forging is an effective route for manufacturing axisymmetric components with significantly higher material utilisation as compared to machining from conventional hot forgings. This paper presents a study on how C263, an alloy system strengthened by γ' , and Inconel 718, an alloy system strengthened by γ'' and δ , deform during the cold rotary forging process and how their microstructures evolve. The two alloys exhibit maximum formability in solution-annealed condition. In this study, both C263 and Inconel 718 were annealed before the cold rotary forging operation. Parts with a 90° bend flange were successfully cold rotary forged from tubular preforms with a wall thickness of 6 mm. For both the alloys, the cold rotary forged parts exhibit significant differences in material properties from the undeformed sections to the most deformed section (i.e. the flanges). Post-forging heat-treatments are required to impart the desired material properties throughout the part. Therefore, appropriate annealing and aging treatments were identified for each of the two alloys. These heat-treatments led to uniform material properties for both deformed and undeformed sections of the cold rotary forged flanges in case of both the alloys.

© 2020 The Authors. Published by Elsevier Ltd.

This is an open access article under the CC BY-NC-ND license (<https://creativecommons.org/licenses/by-nc-nd/4.0/>)
Peer-review under responsibility of the scientific committee of the 23rd International Conference on Material Forming.

Keywords: Cold rotary forging; C263; Inconel 718; Microstructure

1. Introduction

Rotary forging is an incremental bulk forming process where a preform is deformed, at room temperature, into a near net shape part. It has a significant advantage of materials savings (up to 80%) over conventional route of machining from forgings or bar stock to achieve an intricate rotationally symmetric part. Researchers and engineers have been working on the development of rotary forging process for some 100 years now – with E.E Slick being credited with developing the rotary forge process in the period 1906-1922, with the first machine being developed in 1918 [1]. Rotary forging machines have different operational configurations, such as spin-nutation and spin-precession. In case of the spin-nutation, the work-piece is locked in the bottom die where it rotates in unison with

the bottom die about its axis. The top die, tilted at various nutation angles (in some machines this is fix), is moved downward to make contact with the work piece to perform the incremental forming operation (i.e. Rotary forging). In case of spin-precession configuration, the top die moves in orbital (precession) manner along its own axis and brought in contact with the rotating work piece in similar manner as the previous case. In some cases of the orbital type configuration, the bottom die is fixed and as a result, only the top die moves in orbital manner about its axis and deforms the work piece. Rotary forging has been researched by many to understand the mechanisms of the process and how its varying parameters interact with one another [1]. Alloy steels have been most common choice for rotary forging due to their wide-ranging applications and requirements for axisymmetric parts. Several

2351-9789 © 2020 The Authors. Published by Elsevier Ltd.

This is an open access article under the CC BY-NC-ND license (<https://creativecommons.org/licenses/by-nc-nd/4.0/>)
Peer-review under responsibility of the scientific committee of the 23rd International Conference on Material Forming.

10.1016/j.promfg.2020.04.296

researchers have studied this process mainly focusing on process modelling and microstructural evolution. For example, studies have focused on modelling the cold rotary forging of alloy steels and its varying mechanisms [2, 3] as well as to understand material behaviour during the flaring process [4]. Besides the steels, the nickel-based alloys such as C263 and Inconel 718 (IN718) have attracted research in this area due to its widespread application in manufacture of aero engine components. Alloy C263 has high strength up to 816°C and excellent oxidation resistance up to 982°C, therefore it is used in production of gas turbine rings, low temperature combustors, engine-casing parts. C263 can easily be formed by cold working due to its good formability and ductility in annealed condition [5]. On the other hand, gas turbine engine parts, cryogenic tanks, springs, fasteners, pumps, valves and tooling are often made of IN718 due to its excellent creep-stress rupture strength, good corrosion resistance and a service temperature up to 650°C [6]. Several researchers have already attempted rotary forging of IN718 in the temperature range of 950°C – 1100°C, whereas the current authors successfully rotary forged IN718 flanges in cold condition (~20°C – 120°C) [7]. This particular research focuses on studying evolution of microstructural properties and of the two different alloy systems, the C263 and the IN718, in context of rotary forging 90° bend flanges from hollow cylindrical preforms in cold condition. This work is a part of a collaborative research and development programme between Advanced Forming Research Centre (AFRC), University of Strathclyde and Rolls-Royce Plc., where experimental trials were carried out on AFRC’s MJC 200T-4 rotary forge as shown in Fig. 1.

C263, the solution annealing was undertaken at 1150°C, whereas the IN718 was annealed in the range of 950°C – 980°C in order to take the advantage of precipitation hardening. The asR bars were hollowed out with wire EDM to produce a tubular preform with a 6 mm wall thickness. The preform was inserted inside the bottom tool, which has a relevant hollow section to receive the preform with a tight fit to avoid slippage. This provides a synchronous velocity during the rotary forging operation. The conical top tool of the MJC 200T-4 rotary forging machine was then brought in contact with the preform, initially at a shallow nutation angle of between 0-10° to start flaring out the hollow preform. The nutation angle was then gradually increased such that the top tool further deformed (flared out) the wall of the hollow preform and eventually laid it (relevant part of the outer diameter surface of the preform) over the bottom tool surface to achieve the 90° flange. During this experiment, both materials have been cold rotary forged with identical process parameters (such as tool cone angle, flaring angle, feed rate, nutation method, nutation angle, nutation feed rate and spindle velocity). This approach ensured the final flange section to be comparable between the two materials with different ductility, when subjected to a specific set of parameters. A LAND ARC radiometric thermal process imager was used to measure any temperature rise of both the flanges during cold rotary forging. The process was started at the room temperature; however, some increase in temperature occurred due to the friction between the preform and the tool surfaces. Both the C263 and the IN718 rotary forged part flanges reached a maximum temperature of ~100°C and 130°C respectively during cold rotary forging as demonstrated in a Temperature vs. Time graph in Fig. 2.

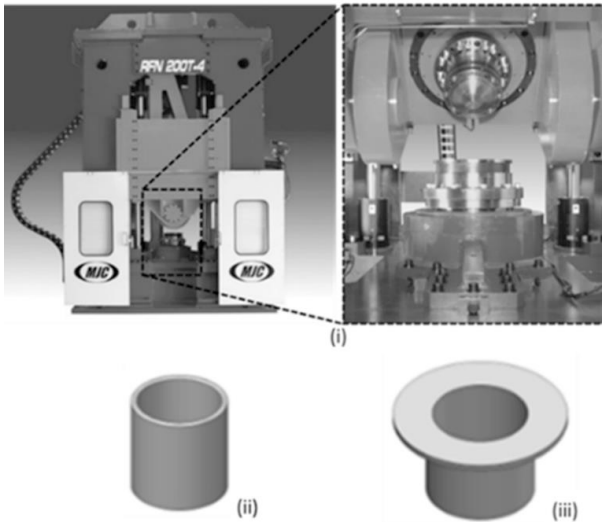


Fig. 1. (i) AFRC's MJC 200T-4 rotary forge test rig, (ii) cylindrical preform, (iii) formation of 90° bend flange using cold rotary forging

2. Cold rotary forging of C263 and IN718

Table 1 shows the material compositions for both solution-annealed C263 and IN718 cylindrical billets (each having 4 inches diameter and 4.7 inches length), which are termed as the ‘as-received’ in this work (hereafter referred as ‘asR’). For the

Table 1. Chemical composition of IN718 and C263 as-received bars

Elements (Wt%)	IN718	C263
Ni+Co	50 – 55	Balance
Cr	17 – 21	19 – 21
Mo	2.8 – 3.3	5.6 – 6.1
Al	0.3 – 0.7	0.3 – 0.6
Ti	0.7 – 1.15	1.9 – 2.4
C	0.02 – 0.08	0.01 – 0.08

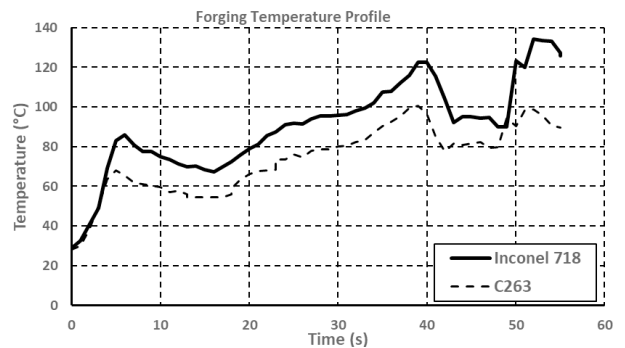


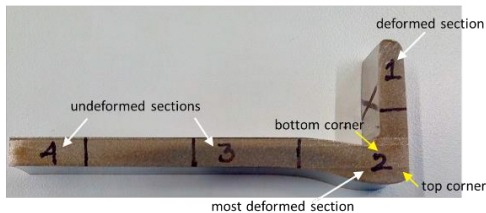
Fig. 2. Temperature profile during cold rotary forging of C263 and IN718 flanges

3. Experimental details

Different annealing treatments followed by aging heat-treatments were applied on the cold rotary forged C263 and IN718 parts in order to achieve a homogeneous microstructural distribution throughout the flange for meeting the hardness requirement as per the respective material specifications (≥ 250 HV for C263 and ≥ 361 HV for IN718). This hardness requirement is an indication of the material strength essential for the service-life. The post-forging heat-treatment of C263 involved – (i) annealing at 1080°C for 15 minutes/air cooling, (ii) followed by aging at 800°C for 8 hours/air cooling. Similarly, cold rotary forged IN718 flange experienced – (i) annealing at 980°C for 30 minutes, (ii) followed by aging at 720°C for 8 hours with a cooling to 620°C at 50°C/hour rate, (iii) followed by 8 hours air cooling from 620°C. Both the cold rotary forged flanges (hereafter termed as ‘CF’) and the cold rotary forged and heat-treated flanges (hereafter termed as ‘CF+HT’) were cut into appropriate slices by wire EDM. Fig. 3 shows the CF and the CF+HT slices, which were further cut into smaller sections 1 – 4 for microstructural, hardness and surface roughness analysis. The C263 sections were etched using Glyceregia (ASTM standard no 87). The IN718 asR and CF sections were electro-etched with 10% oxalic acid, whereas micro etch was used to reveal the microstructure in CF+HT sections [7].

Leica DM1200M was used to capture the micrographs from each sections as shown in Fig. 3a, and the respective grain size analysis was done according to ASTM standard E112 – 13. A Struers hardness tester was used to measure the hardness of these sections using Vicker’s indenter with a fixed load of 1 kgf according to ASTM standard E384 – 17. Fig. 3b shows the surfaces on CF and CF+HT slices for roughness measurement using Alicona Infinite Focus IFM G4 surface profilometer. Each line scan provides Ra (arithmetic mean deviation of the assessed profile), Rq (root mean square value) and Rz (average distance between the highest peak and lowest valley in each sampling length) values.

(a) Nomenclatures for microstructural and hardness analysis:



(b) Nomenclatures for surface roughness analysis:

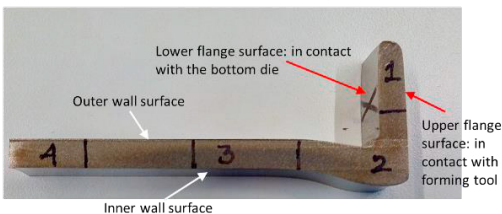


Fig. 3. Schematic diagram for cutting and preparation of CF and CF+HT sections 1 – 4 for (a) microstructural, hardness and (b) roughness analysis

4. Results and Discussion

4.1. Microstructure

Fig. 4 shows representative optical images as collected from both the C263 and IN718 asR cross-sections. The C263 microstructure shows presence of an equiaxed grain structure including many twins with an average grain size of $\sim 113 \mu\text{m}$ (Fig. 4a), whereas IN718 microstructure is consisted of substantially smaller equiaxed grains with an average grain size of $\sim 12.6 \mu\text{m}$ (Fig. 4b). Cold rotary forging results in a microstructural variation throughout the flange part, where sections 1 and 2 experience the deformation due to direct contact with the forming tool but sections 3 and 4 remain unaffected. Thus, the microstructure observed at the most deformed and the one of the undeformed sections, i.e. sections 2 and 4 respectively, are considered for detailed analysis in this study for both the materials.

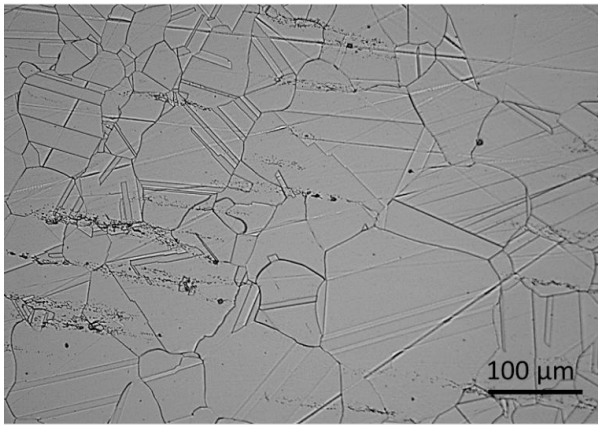
Fig. 5 shows the representative microstructure from the IN718 CF and CF+HT sections 2 and 4 respectively. Equiaxed grains with several twins are evident in the undeformed CF section 4, whereas most of the deformed CF section 2 exhibits elongated grain structure, strong evidence suggesting that the section would have undergone significant deformation due to the constraints of the rotary forging process. After heat-treatment, the undeformed CF+HT section 4 retains the equiaxed grain structure showing no traces of carbides. The elongated grains observed in the most deformed CF section 2 are transformed into equiaxed grains because of the heat-treatment. The heat-treatment results in an overall homogeneous microstructure throughout the IN718 CF+HT flange, a desirable outcome of isotropic properties from manufacturing point of view. It should be noted here that the annealing is used to recrystallize and homogenise the microstructure, whereas the double aging is chosen in order to impart the formation of both γ' and γ'' phases.

To visualise the microstructural evolution, the C263 flange micrographs for CF and CF+HT conditions are shown in Fig. 6. The most deformed section 2 in the C263 CF flange shows a transition (transition zone is annotated with a dashed line) of microstructure from elongated grains towards section 1 to the relatively equiaxed grains towards section 3, particularly at the top corner. At the bottom corner of section 2, the microstructure consists of mainly large elongated grains. On the other hand, the undeformed C263 CF section 4 shows random equiaxed grain structure with a lot of twins. The heat-treatment chosen for C263 helps to impart a recrystallized and homogenised microstructure with γ' as the main strengthening phase [8]. The heat-treatment refines the CF microstructure; however, the random grains remain. The refinement is significant in particularly CF+HT section 2 due to the formation of many deformed small grains; although the twins are not fully eliminated. The refinement is also noticeable for CF+HT section 4, which shows a comparatively homogeneous microstructure with relatively less presence of twins.

Fig. 7 summarises the average grain size in asR, CF and CF+HT sections from both C263 and IN718 flanges. The solid and shaded colour bars are used to represent C263 and IN718 sections respectively and the image in the inset shows the

different sections taken into account during grain size measurement. It should be noted that the IN718 sections show minor variation in average grain size after cold rotary forging as compared to asR microstructure, but this is completely eliminated after heat-treatment. On the other hand, C263 sections shows significant variation in average grain size after cold rotary forging particularly compared to asR microstructure. After the heat-treatment, formation of equiaxed grains minimises this variation, leading to average grain size smaller than that of the asR microstructure. Overall, the IN718 flange sections show noticeably more retention of the microstructure homogeneity throughout the rotary forging process stages, as compared to those of the C263.

(a) C263 asR cross-section



(b) IN718 asR cross-section

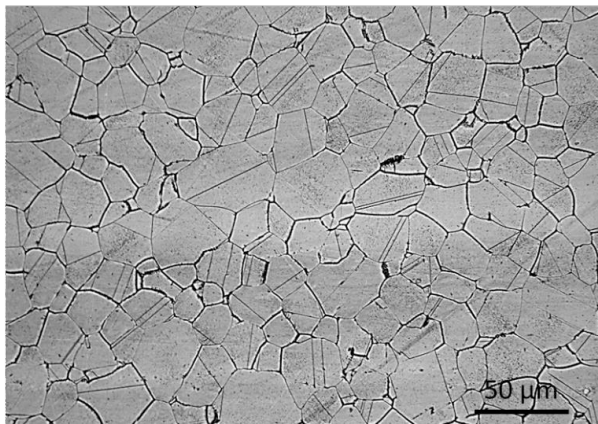
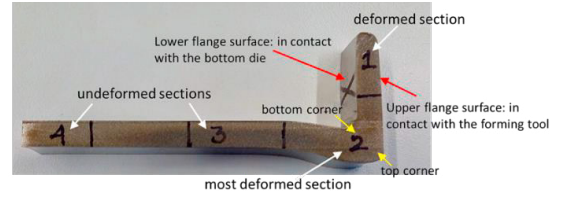
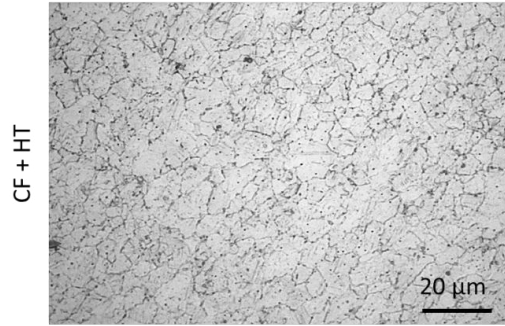
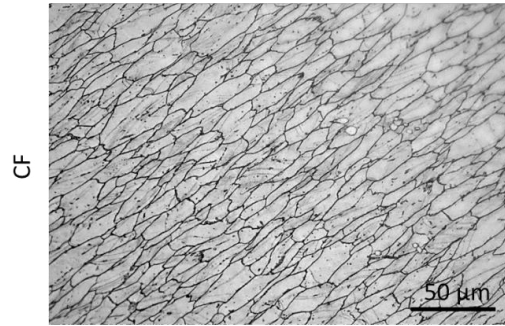


Fig. 4. Representative microstructure of the asR materials along the cross-section – (a) C263 and (b) IN718



section2 (most deformed)



section4 (undeformed)

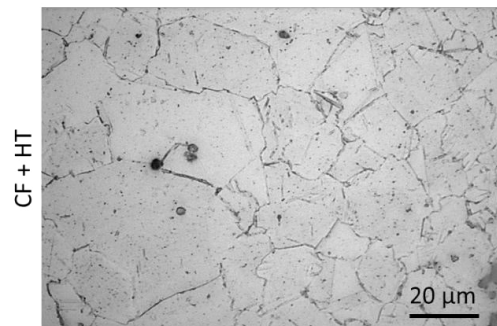
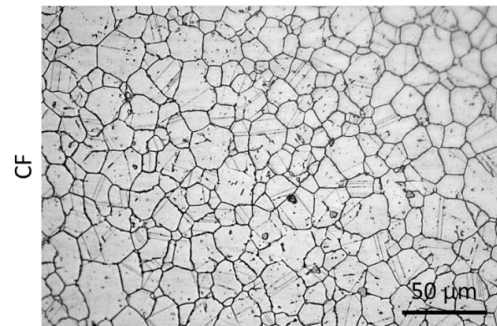


Fig. 5. Representative microstructure of the IN718 CF and CF+HT most deformed and undeformed sections

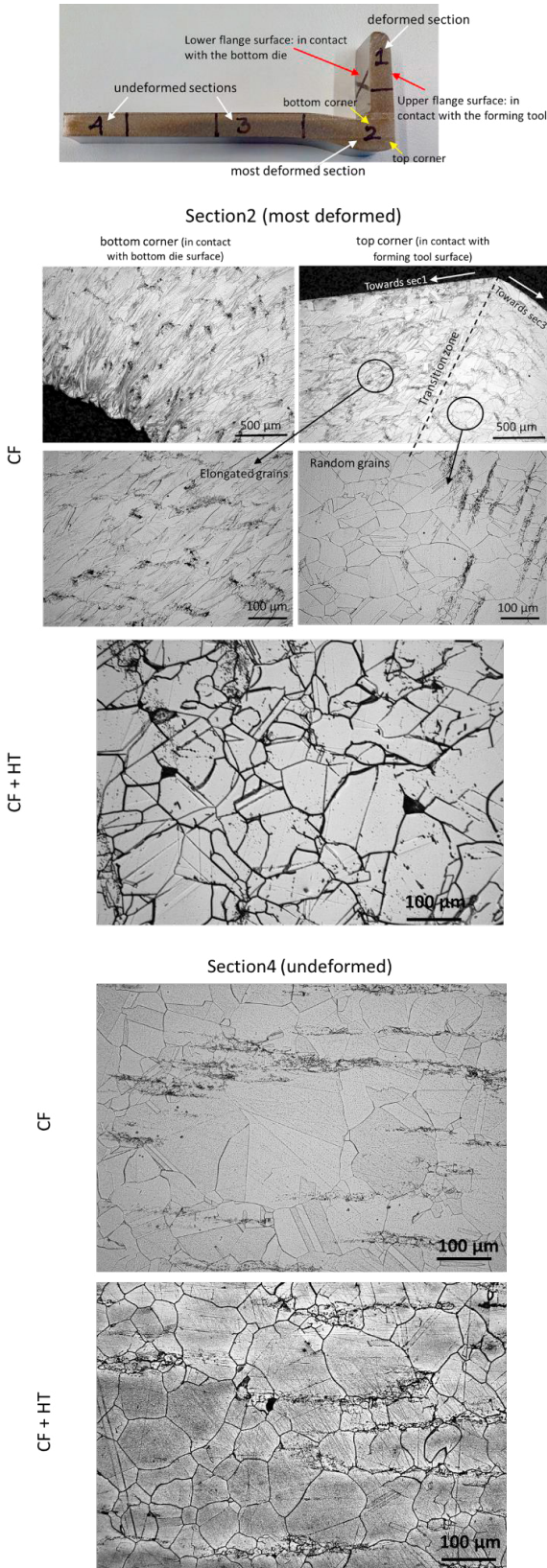


Fig. 6. Representative microstructure of the C263 CF and CF+HT most deformed and undeformed sections

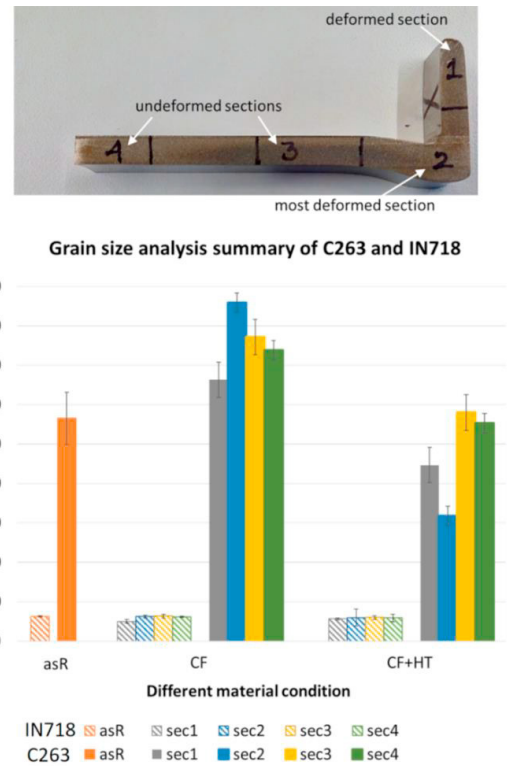


Fig. 7. Summary of average grain size in asR, CF and CF+HT sections from both C263 and IN718 flanges

4.2. Hardness

Fig. 8 summarises the average micro hardness values in asR, CF and CF+HT sections from both C263 and IN718 flanges. The solid and shaded colour bars are used to represent C263 and IN718 sections respectively. The image in the inset shows the different sections taken into account during hardness measurement. The asR C263 and IN718 materials show an average hardness of ~188 HV and ~267 HV respectively, which is dependent on their different initial microstructure. After cold rotary forging, both materials show a significant variation in the average hardness of CF sections, where both sections 1 and 2 show more than twice as much increase in the average hardness values due to formation of highly deformed elongated grain structure as compared to the undeformed sections 3 and 4. The heat-treatment introduces a uniform homogeneous microstructure throughout the IN718 CF+HT flange showing no significant grain refinement (Fig. 7) and therefore provides a uniform hardness distribution, which is mainly attributed to the γ' precipitation hardening [7]. Similarly for C263, the uniform hardness distribution in CF+HT sections is a combination of both precipitation hardening by γ' and refinement of the random equiaxed microstructure as observed in CF sections. It should be noted here that both C263 and IN718 CF+HT flanges show an average hardness >280 HV and >380 HV, therefore meeting the hardness requirements as per the respective material

specifications (≥ 250 HV for C263 and ≥ 361 HV for IN718 respectively).

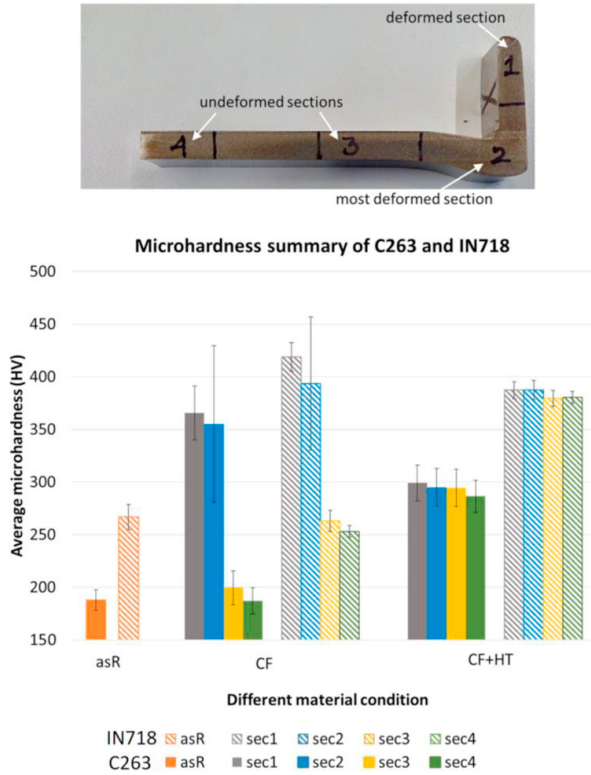


Fig. 8. Summary of average micro hardness in asR, CF and CF+HT sections from both C263 and IN718 flanges

4.3. Surface Roughness

Fig. 9 summarises the average roughness values in asR, CF and CF+HT sections from both C263 and IN718 flanges. The solid and shaded colour bars are used to represent C263 and IN718 sections respectively. The image in the inset shows the different surfaces taken into account during linear roughness measurement, i.e. (i) upper flange surface (in contact with the forming tool), (ii) lower flange surface (in contact with the bottom die), (iii) outer wall surface and (iv) inner wall surface. For both materials, a significant improvement in Ra value is observed after cold rotary forging when compared to asR condition. After heat-treatment of the CF flanges, a slight deterioration in Ra value is noted for both the materials. The trend is found similar for Rq and Rz values. Overall, the CF+HT flanges have smooth surface finish that has the potential to be left as formed in a final part.

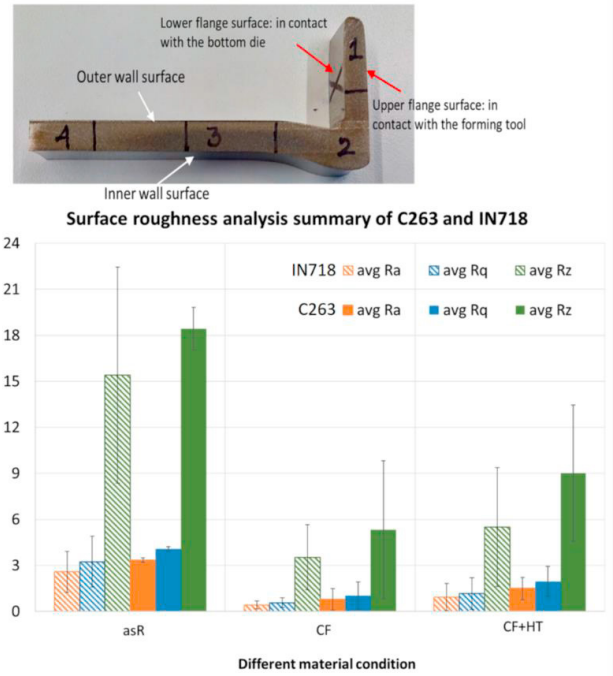


Fig. 9. Summary of average surface roughness parameters in asR, CF and CF+HT sections from both C263 and IN718 flanges

5. Conclusions

Following conclusions are drawn from this work:

- Both the C263 and the IN718 can be cold rotary forged into near net-shape axisymmetric component with a 90° bend flange. The solution-annealed condition of the preform is found to be suitable for cold rotary forging operation for both materials.
- Cold rotary forging leads to a deformed microstructure with elongated grains in the bend section resulting in a significant hardness variation between deformed and undeformed sections. This inconsistency in hardness distribution can be overcome by suitable heat treatments to restore homogeneity. A combination of annealing and aging treatments suitable for these two different alloys have been found to be effective in achieving the microstructure homogeneity and hardness uniformity.
- The adequate hardness observed in the heat-treated flanges is attributed to the formation of main strengthening phases γ' and γ'' for C263 and IN718 respectively, where refined microstructure also plays an important role. Besides this, a slight deterioration of the surface finish is observed after heat-treatment, although it is well within the acceptable range.
- Overall, the IN718 exhibits marked retention of the microstructure homogeneity, in terms of grain size variation, throughout the rotary forging process stages inclusive of heat treatments as compared to the C263, which shows significant variations. However, through suitable heat treatments, desirable properties can successfully be achieved in both the alloys.

Acknowledgement

The authors would like to acknowledge Rolls Royce Plc for funding this work from their Innovate UK: Aerospace Technology Institute Strategic R&D Project grant (application no. 66733-263147) titled “Manufacturing Portfolio Project 2: Manufacture of Advanced Materials”.

References

- [1] Standring P. Characteristics of rotary forging as an advanced manufacturing tool. Proceedings of the Institution of Mechanical Engineers, Part B: Journal of Engineering Manufacture 2001; 215 (7): 935-945.
- [2] Krishnamurthy B, Bylya O, Muir L, Conway A, Blackwell P. On the Specifics of Modelling of Rotary Forging Processes. Computer Methods in Materials; 2016.
- [3] Han X, Hua L. Friction behaviors in cold rotary forging of 20CrMnTi alloy. Tribology International 2012; 55: 29–39.
- [4] Perez M. Analysis of innovative incremental cold forming process for the manufacturing of aerospace rotating parts. 12th International Manufacturing Science and Engineering Conference; 2017.
- [5] NeoNickel. A precipitation-hardenable nickel-chromium-cobalt alloy, Alloy C263 exhibits excellent high-temperature strength up to 816°C. [Online]. Available: <https://www.neonickel.com/alloys/nickel-alloys/alloy-c263/>. [Accessed 22 2019].
- [6] NeoNickel. A precipitation-hardenable nickel-chromium grade, Alloy 718 is a high strength superalloy used at temperatures up to 648°C. [Online]. Available: <https://www.neonickel.com/alloys/nickel-alloys/alloy-718/>. [Accessed 11 2019].
- [7] Mandal P, Lalvani H, Tuffs M. Cold Rotary Forging of Inconel 718. Journal of Manufacturing Processes 2019; 46: 77-99.
- [8] Maier G, Hubsch O, Riedel H, Somsen C, Klower J, Mohrmann R. Cyclic plasticity and lifetime of the nickel-based Alloy C-263: Experiments, models and component simulation. EURO SUPER ALLOYS 2014; 2014.